Band-Pass Filter Design by Segmentation in Frequency Domain for Detection of Epithelial Cells in Endomicroscope Images

Bastian Bier[1], Firas Mualla[1], Stefan Steidl[1], Christopher Bohr[2], Helmut Neumann[3], Andreas Maier[1], Joachim Hornegger[1]

[1]Pattern Recognition Lab
[2]Department of Otorhinolaryngology
[3]Department of Medicine I
Friedrich-Alexander-Universität, Erlangen-Nürnberg, Germany
bastian.bier@fau.de

Abstract. Voice hoarseness can have various reasons, one of them is a change of the vocal fold mucus. This change can be examined with micro endoscopes. Cell detection in these images is a difficult task, due to bad image quality, caused by noise and illumination variations. In previous works, it was observed that the repetitive pattern of the cell walls cause an elliptical shape in the Fourier domain [1, 2]. A manual segmentation and back transformation of this shape results in filtered images, where the cell detection is much easier [3]. The goal of this work is to automatically segment the elliptical shape in Fourier domain. Two different approaches are developed to get a suitable band-pass filter: a thresholding and an active contour method. After the band-pass filter is applied, the achieved results are superior to the manual segmentation case.

1 Introduction

A hoarse voice can have various reasons, such as structural changes or changes in the mucus of the vocal folds, leading to an influence on the voice signal [4]. One method to examine the vocal fold mucus is to use micro endoscopes in vivo and investigate the resulting epithelial cell images. Compared to normal microscopes, micro endoscope images have a poor image quality with much noise and brightness changes across the image. This lack of image quality makes the detection of cells a difficult task.

In the literature, several cell detection approaches exist [5, 6, 7, 8]. The cell images we use have the property that no separation of background and foreground has to be done, because cells cover the whole scene. Furthermore, the cell walls form a repetitive pattern. This property is used in [1, 2], where they observed a circular shape in the Fourier domain of cell images, representing the pattern of the cell walls in the image. Furthermore, this approach is used in [3], where the ellipse is segmented manually in the Fourier domain. The filtered cell

H. Handels et al. (Hrsg.), *Bildverarbeitung für die Medizin 2015,* Informatik aktuell,
DOI 10.1007/978-3-662-46224-9_71, © Springer-Verlag Berlin Heidelberg 2015

image has less noise and cell detection is then easier and more robust. The goal of this work is to find a method which automatically segments the elliptical shape in the Fourier domain. Two different methods are presented: one thresholding approach and an approach using geodesic active contour segmentation.

2 Material and methods

Nine images of epithelial cells of the vocal fold acquired with a micro endoscope of a Cellvisio probe-based confocal laser endomicroscope (pCLE) system are used in this work, same images as in [3] (Fig. 1(a)). In order to avoid artificial frequencies of the black circle around the cells, the original images are cropped (Fig. 1(b)). Image resolution after cropping is 405×397 pixels. In Fig. 1(c), the Fourier transform of the cropped image is shown. In the middle of the image, one can see clearly an elliptical shape corresponding to the repetitive pattern of the cell walls. The following presented methods segment this circle to get a band-pass filter mask. The methods are implemented in C++ with ITK [9]. Cell detection is performed by detecting intensity minima in the filtered image.

2.1 Labeling of the reference data and evaluation

To be able to evaluate the new methods, ground truth is needed. This is done by manually labeling the cropped cell images with the program ImageJ. In the labeling procedure, each cell center is clicked and the coordinate of these reference cells are stored. These coordinates are used for evaluation.

Due to the bad image quality caused for example by dirt on the lens and illumination changes, it is not easy to recognize all cells properly during the labeling process. Consequently, one has to have in mind that even the ground truth contains some mistakes. The average number of cells per image after cropping is 294.

In order to be able to evaluate the methods quantitatively, the detected cells have to be matched with the reference cells. This is done with a standard

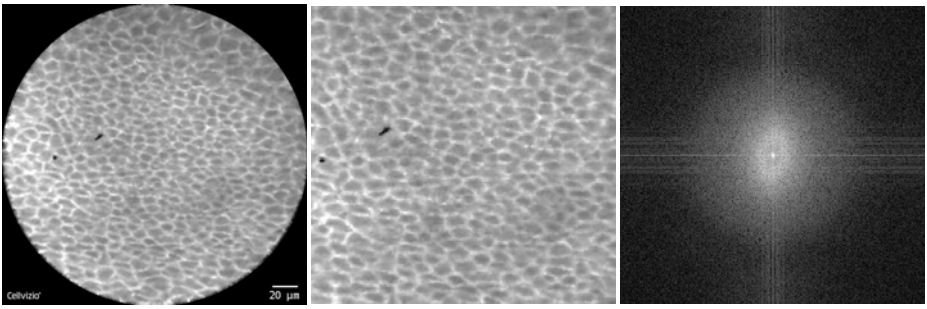

(a) Epithelial cell image (b) Cropped input image (c) Fourier transform of (b)

Fig. 1. Sample epithelial cell image and its Fourier transform. In the Fourier transform an elliptical shape in the center of the image can be seen.

algorithm for such problems, the Hungarian algorithm. This matching algorithm allows a maximum distance of 8 pixels between the reference and the detected cells. This is the same evaluation method used in [3].

2.2 Thresholding method

The thresholding method is based on finding a suitable threshold. Experimentally, a relative threshold of 0.988 is estimated, meaning that the highest 1.2% of the values in the Fourier image are set to one, and the other 98,8% to zero

$$M(\mathbf{x}) = \begin{cases} 1 & \text{if } |F(\mathbf{x})| > \text{threshold} \\ 0 & \text{otherwise} \end{cases} \tag{1}$$

$M(\mathbf{x})$ describes the mask at coordinate $\mathbf{x}$ and F is the input Fourier image. After applying this threshold, many pixels inside the elliptical shape are zero (Fig. 2(a)). In order to get a nice ellipse, a median filter with size 12 is used to smooth the pixel cloud. The brightness and illumination changes in the images can be reduced by cutting out the low frequencies. This is done by setting a circle with radius of three pixels in the center of the image mask to zero. The resulting band-pass filter mask is shown in Fig. 2(b).

2.3 Geodesic active contours segmentation

The geodesic active contour filter needs a feature image on which it can find a contour iteratively, according to the energy term [10]

$$\frac{d}{dt}\Psi = -\alpha \mathbf{A}(\mathbf{x}) \cdot \nabla\Psi - \beta B(\mathbf{x})|\nabla\Psi| + \gamma Z(\mathbf{x})\kappa|\nabla\Psi| \tag{2}$$

$\mathbf{A}(\mathbf{x})$ describes the advection term to the edge in the image, $B(\mathbf{x})$ describes the propagation term and $Z(\mathbf{x})$ is the spatial modifier term for the mean curvature κ. α, β and γ are weights defining the influence of each term. The algorithm then finds the optimal contour, where the level-set function Ψ equals 0.

To get a feature image, a filter is used which calculates the gradient of the image by convolving it with the first derivative of the Gaussian. The smoothing size of the Gaussian is determined experimentally and set to $\sigma = 0.9$ (Fig. 2(c)). Afterwards, the derivative image is multiplied by -1 and scaled between zero and one, as required for the geodesic filter. For Eq. (2) this results that $B(\mathbf{x})$ and $Z(\mathbf{x})$ are equal to the the negative and scaled gradient magnitude image. $\mathbf{A}(\mathbf{x})$ is the negative gradient of the feature image. The geodesic active contour filter is then applied with the weights $\beta = 1.0$, $\gamma = 1.0$ and $\alpha = 4.0$. Furthermore, the filter needs an initial contour, set here to a circle around the center of the image with a radius of 24 pixels. Same as in the thresholding method, the low frequencies are cut out of the mask center with a circle of radius three pixels. The resulting band-pass filter mask is shown in Fig. 2(d).

Table 1. Recall, Precision and the F-measure results averaged over all images.

Method	Recall	Precision	F-measure
Original Images	98.2 ± 0.9	24.3 ± 4.0	38.8 ± 5.1
Manual Segmentation [3]	94.6 ± 3.7	70.0 ± 7.3	80.2 ± 4.7
Thresholding Method	83.6 ± 2.2	83.9 ± 3.3	83.7 ± 2.0
Geodesic Segmentation	83.5 ± 5.1	83.1 ± 4.1	83.3 ± 4.1

3 Results

In Tab. 3, the results achieved with the thresholding and the geodesic method are compared with minima detection on the original unprocessed image and with the results of the manual segmentation presented in [3]. The two presented methods achieved almost the same results. In addition, they were considerably superior to minima detection on the unprocessed image and approximately 3% better than [3] in F-measure.

Qualitative results are shown in Fig. 3. In Figs. 4(a) and 4(b), the cell image before and after the processing is shown with a zoomed region of the same ROI

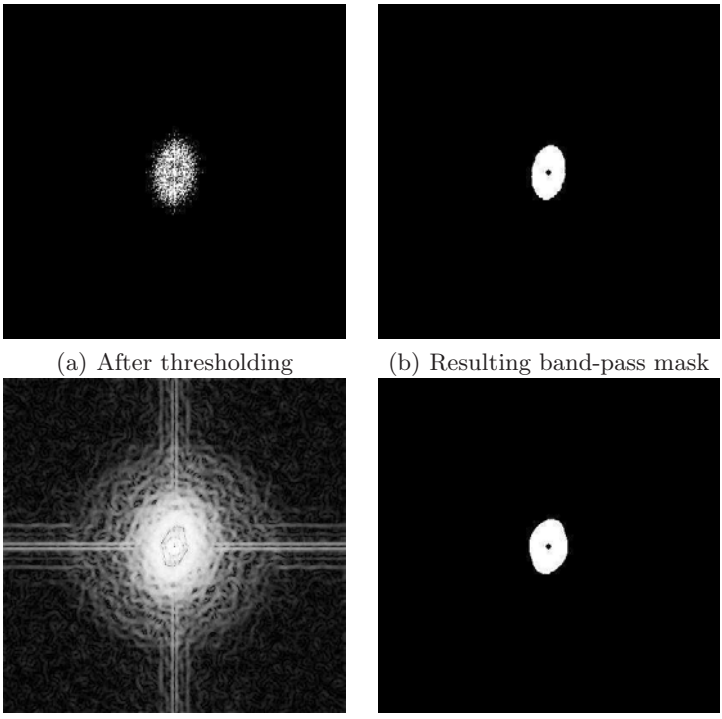

(a) After thresholding (b) Resulting band-pass mask

(c) After gradient filtering (d) Resulting band-pass mask

Fig. 2. Intermediate steps and final masks of the thresholding method (upper row) and the geodesic segmentation (lower row).

Fig. 3. Qualitative comparison between minima detection on an unprocessed image and on an image filtered with the band-pass filter designed by the thresholding method. In Figs. 4(c) and 4(d), reference cells are marked with a red plus sign and the automatically detected cells with a green plus sign. The yellow lines in Fig. 4(d) connect matched cells.

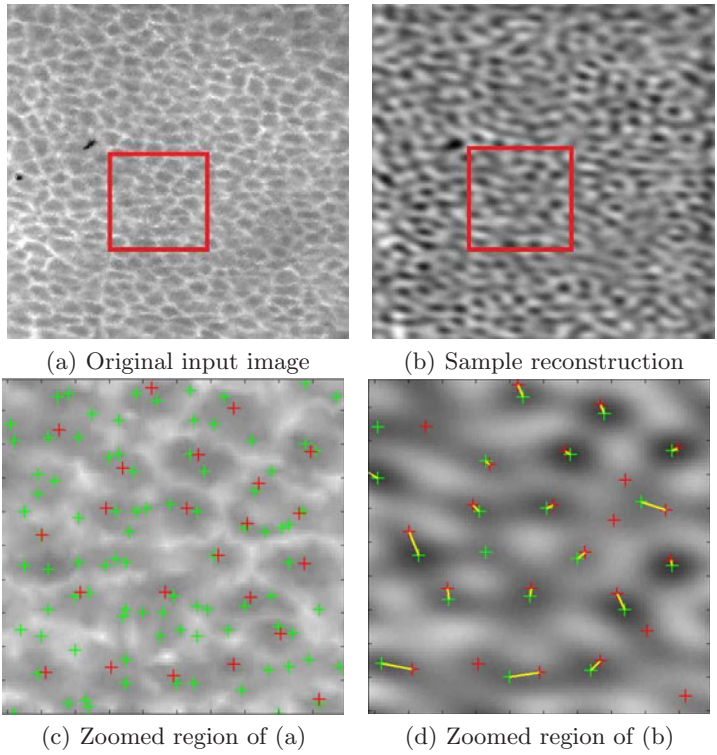

(a) Original input image (b) Sample reconstruction

(c) Zoomed region of (a) (d) Zoomed region of (b)

(Fig. 4(c) and 4(d)). Here, one can see that the band-pass filtered image contains less noise and the cell walls and centers are well visible.

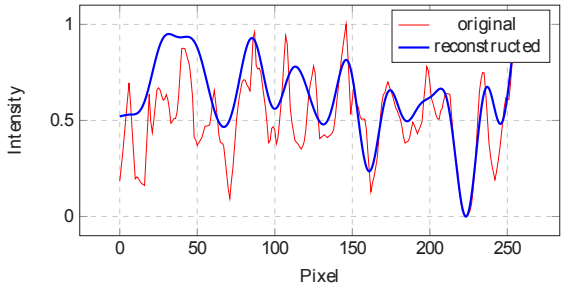

Fig. 4. Line profile comparison of the original and the reconstructed image.

The effect of the enhanced cell walls can be seen in Fig. 4, where two normalized line profiles of the original and the reconstructed image are shown. The noise is removed and only the cell walls remain.

4 Conclusion

In [3], it was shown that detection of epithelial cells in endomicroscope images of the vocal folds is possible with basic image processing techniques when an image is preprocessed with a band-pass filter which corresponds to the repetitive pattern of cells inside the image. In this paper, we showed that it is possible to automatically design this filter by segmenting an ellipse which shows up in Fourier domain, even though segmentation parameters were manually set or experimentally found.

References

1. Ruggeri A, Grisan E, Jaroszewski J. A new system for the automatic estimation of endothelial cell density in donor corneas. Br J Ophthalmol. 2005; p. 306–11.
2. Foraccia M, Ruggeri A. Estimating dell density in corneal endothelium by means of fourier analysis. Proc Second Jt EMBS/BMES. 2002; p. 1097–8.
3. Mualla F, Schöll S, Bohr C, et al. Epithelial cell detection in endomicroscopy images of the vocal folds. Proc Int Multidisciplin Microsc Congr. 2013; p. 1097–8.
4. Klemuk SA, Riede T, Walsh EJ, et al. Adapted to roar: functional morphology of tiger and lion vocal folds. PLoS One. 2011;6(11):e27029.
5. Long X, Cleveland W, Yao Y. Automatic detection of unstained viable cells in bright field images using a support vector machine with an improved training procedure. Comput Biol Med. 2006;36(4):339–62.
6. Mualla F, Schöll S, Sommerfeldt B, et al. Automatic cell detection in bright-field microscope images using SIFT, random forests, and hierarchical clustering. IEEE Trans Med Imaging. 2013;32(12):2274–86.
7. Mualla F, Schöll S, Sommerfeldt B, et al. Unsupervised unstained cell detection by SIFT keypoint clustering and self-labeling algorithm. Lect Notes Computer Sci. 2014;8675:377–84.
8. Pan J, Kanade T, Chen M. Heterogeneous conditional random field: realizing joint detection and segmentation of cell regions in microscopic images. Proc IEEE Comput Soc Conf Comput Vis Pattern Recognit. 2010; p. 2940–7.
9. Johnson HJ, McCormick M, Ibáñez L. The ITK Software Guide. 3rd ed.; 2013.
10. Caselles V, Kimmel R, Sapiro G. Geodesic active contours. Int J Computer Vis. 1997;22(1):61–79.